Physics of Fluids

Manipulation of jet breakup length and droplet size in axisymmetric flow focusing upon actuation

Cite as: Phys. Fluids **31**, 091702 (2019); https://doi.org/10.1063/1.5122761
Submitted: 01 August 2019 . Accepted: 06 September 2019 . Published Online: 24 September 2019

Chaoyu Yang, Ran Qiao, Kai Mu, Zhiqiang Zhu, Ronald X. Xu, and Ting Si

Physics of Fluids LETTER scitation.org/journal/phf

Manipulation of jet breakup length and droplet size in axisymmetric flow focusing upon actuation

Cite as: Phys. Fluids 31, 091702 (2019); doi: 10.1063/1.5122761
Submitted: 1 August 2019 • Accepted: 6 September 2019 •
Published Online: 24 September 2019

View Online Export Citation CrossMark

Chaoyu Yang,[1] Ran Qiao,[2] Kai Mu,[2] Zhiqiang Zhu,[1] Ronald X. Xu,[1,3] and Ting Si[2,a)]

AFFILIATIONS

[1]Department of Precision Machinery and Precision Instrumentation, University of Science and Technology of China, Hefei 230026, People's Republic of China
[2]Department of Modern Mechanics, University of Science and Technology of China, Hefei 230026, People's Republic of China
[3]Department of Biomedical Engineering, The Ohio State University, Columbus, Ohio 43210, USA

[a)]**Electronic mail:** tsi@ustc.edu.cn

ABSTRACT

External sinusoidal actuation is employed in the axisymmetric flow focusing (AFF) for generating uniform droplets in the jetting mode. The perturbations propagating along the meniscus surface can modulate the rupture of the liquid jet. Experiments indicate that the jet breakup length and the resultant droplet size can be precisely controlled in the synchronized regime, which are further confirmed by the scaling law. The finding of this study can help for better understanding of the underlying physics of actuation-aided AFF, and this active droplet generation method with fine robustness, high productivity, and nice process control would be advantageous for various potential applications.

Droplets at micron and submicron scales are of great significance in various scientific and engineering applications.[1–5] In the past few decades, emerging microfluidic technologies such as polydimethylsiloxane (PDMS) microchannels,[6–9] glass microcapillaries,[10,11] and flow focusing devices[12–14] have been developed to produce uniform droplets. The Reynolds number of microchannel and microcapillary flows is often far smaller than unity due to small confined walls and low liquid flow rates, resulting in relatively low productivity.[15] The parallelization can be employed to produce droplets with high productivity, but the device integration is usually quite complicated.[16] Differently, flow focusing is able to generate a steady liquid jet moving in an open space,[12–14] which can avoid the capillarity and wetting effects of boundary walls and boost liquid flow rates by hundreds of folds, leading to dramatically increased productivity.[13] The dripping regime is demonstrated to be able to produce highly uniform droplets, but the parametric range is a little narrow.[14,17] The transition from dripping to jetting by further increasing the Reynolds number is an effective and simple way to increase productivity,[18] but the droplet size distribution will become wide and the jet breakup length is time-dependent due to the Rayleigh-Plateau instability.[19–21] The jetting process with rich dynamic phenomena can be affected by many parameters such as the liquid flow rates, viscosities, and interface tension of different fluids.[22] Moreover, a surfactant can be used to stabilize resultant droplets, which makes the jetting regime arise more easily under the same flow parameters.[23]

Active droplet generation has been proposed in microchannel flows by applying external energy, including acoustic, electric, magnetic, or mechanical sources.[3,24,25] External perturbations can be successfully applied on various flows to manipulate the droplet formation processes with desirable frequencies.[26] Most previous studies mainly focused on the microchannel and microcapillary flows, which have been well reviewed.[3,25] Differently, in the axisymmetric flow focusing (AFF) process, the surrounding high-speed flow continuously provides adequate energy input to overcome the interfacial tension and the jetting mode can be easily formed. As the external perturbations are applied, the competition between the additional force and the inertial force on the interface will result in distinct phenomena, which has been demonstrated numerically.[27] However, the experimental evidence for actuation-aided AFF is still lacking. In

this work, we report the first experiment of the jetting regime upon actuation in axisymmetric flow focusing (AFF) and study the effects of process parameters on the breakup length of the liquid jet and the size of resultant droplets quantitatively. When the focused liquid is actuated by mechanical vibration with a sinusoidal signal, the droplet size in the synchronized mode can be precisely determined by the focused liquid flow rate and the vibration frequency, independent of other parameters such as geometries of the AFF device and physical properties of the liquids. Moreover, the jet breakup length can be directly controlled by vibration amplitudes modulated by the meniscus formed in the AFF process. The results would provide a fundamental understanding of the activated AFF process in the jetting regime and will benefit the development of more active techniques for multilayered droplet generation in coflow focusing configurations.[28–33]

The principle of AFF equipped with an actuator is depicted in Fig. 1(a). A needle with an inner diameter of D_i = 1.0 mm and an outer diameter of D_o = 1.2 mm is assembled in the AFF chamber. A polytetrafluoroethylene (PTEF) membrane mounted on the needle inlet can be directly vibrated by a piezoelectric actuator (PSt150VS12, Core morrow, China), which is fixed on an optical table in order to avoid interference with other sections and connected to a signal generator and a power amplifier (HSA4051, NF corporation, Japan) with an output voltage (U). The needle outlet is located with a vertical distance of H = 0.9 mm from the focusing orifice at the bottom plate of the AFF chamber, with an orifice inner diameter of d = 0.8 mm and a bottom plate thickness of l = 1.0 mm. Figure 1(b) presents the simple structure of the activated AFF device in experiments, which can be easily assembled and adjusted. Two optical windows are mounted on both sides of the AFF chamber for convenient observation. A collector with its top cover open is filled with focusing liquid and placed at the bottom of the AFF device. In order to ensure the repeatability and reliability of the system, we have manufactured the needle and the AFF chamber with stainless steel by the computerized numerical control method. Two syringe pumps (WK-101P, Nanjing Anerke Electronics Technology, China) are used to provide continuous flows of the focused and focusing liquids through two channels connected to the needle and the chamber side wall, respectively. The jet dynamic behaviors are monitored by a high-speed video camera (AX200, Photron, Japan) equipped with a microscopic lens (Z16, Leica, Germany) under illumination of a light-emitting diode (LED) light source (U-40T, DannyU, China). The harmonic vibration features of the meniscus are obtained with an image processing program developed with MATLAB. The droplet size is analyzed with Image-Pro Plus 6.0. For the fundamental study, silicone oil (10 cSt, 50 cSt, and 100 cSt, Clearco, America) and deionized water (Direct-Q 3, Millipore, America) are chosen as the focused and focusing liquids, respectively. The density and viscosity of deionized water are 995 kg/m^3 and 1.0 cSt, respectively. The densities for 10 cSt, 50 cSt, and 100 cSt silicone oil are 930 kg/m^3, 960 kg/m^3, and 965 kg/m^3, respectively. All experiments are performed at room temperature of 25 °C.

In a typical actuated AFF process, the focused fluid with a constant flow rate (Q_1) passes through the channel to the needle, where the PTEF membrane is excited by the piezoelectric actuator with applied voltage (U) to guarantee the sinusoidal reciprocating motion with an initial frequency (f_e) and an amplitude (ε_0). The focusing liquid with a constant flow rate (Q_2) is supplied continuously to the chamber, accelerating the focused liquid to form the meniscus between the nozzle and the orifice. The liquid jet emitting from the meniscus tip moves through the orifice and eventually breaks up into droplets due to the perturbation propagation along the jet surface. Different from traditional microchannel flows, the Reynolds numbers in AFF can be up to the order of 100, and the liquid jet moving outside the orifice in an open space has a much larger velocity than that confined in microchannel walls.[13,15] Besides, the meniscus formation at higher liquid flow rates in AFF can improve the robustness of the process and the breakup of the liquid jet is nearly independent of geometrical parameters of the device.[12,18] More interestingly, the meniscus exhibits a regular harmonic vibration under excitation, as demonstrated in Fig. 2(a). The dynamic process of the meniscus is clearly recorded by the high-speed photography, as shown in Video S1 of the supplementary material. We extract the meniscus boundary by MATLAB image processing, choose one point on the meniscus surface [e.g., the point P near the orifice entrance in the inset image

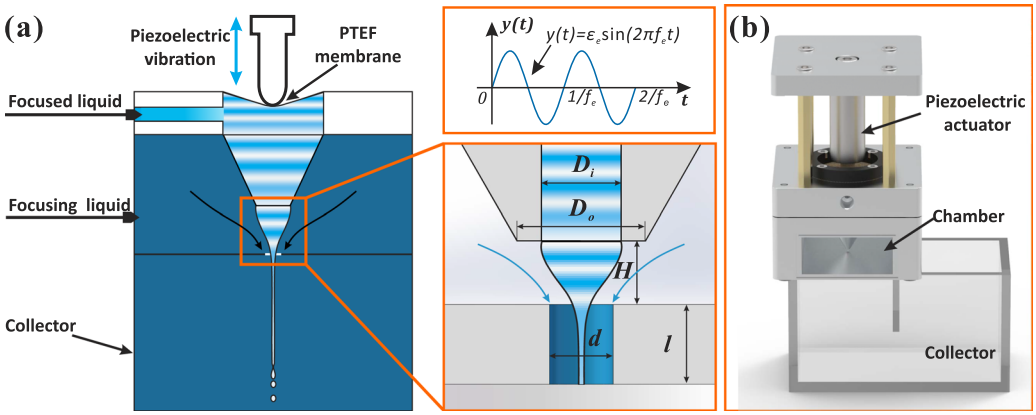

FIG. 1. (a) Schematic of AFF principle with mechanical vibration acting on the focused liquid. (b) Experimental structure of the activated AFF device mainly involves a piezoelectric actuator, an AFF chamber, and a bottom collector.

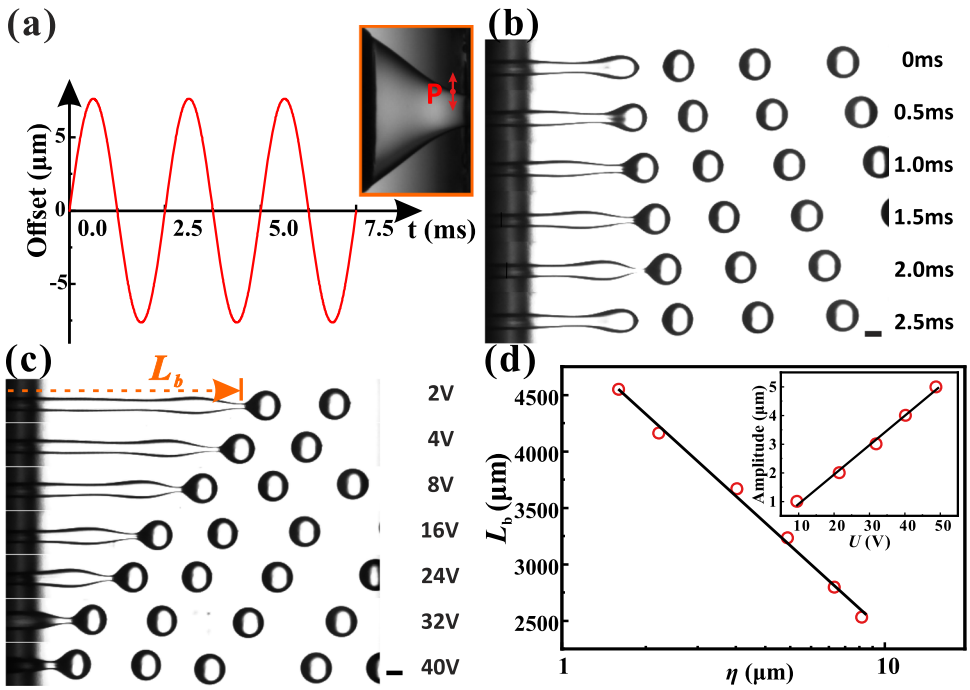

FIG. 2. (a) The harmonic vibration on the meniscus surface (point P in the inset). (b) The sequence of images showing the breakup process of a liquid jet during one period (2.5 ms) with a fixed voltage (U = 16 V). (c) Typical photographs of the liquid jet with an increase in the value of U (2–40 V). (d) The jet breakup length (L_b) vs vibration amplitude (y) at point P. (The inset shows the linear relationship between the external perturbation amplitude ε_0 and the applied voltage U.) In all experiments, Q_1 = 50 ml/h (50 cSt silicone oil), Q_2 = 2000 ml/h (deionized water), and f_e = 400 Hz. Scale bar: 200 μm.

of Fig. 2(a)], and distinguish the offset of perturbations at the point. It can be easily seen that the vibration curve follows strict sinusoidal shape and its frequency is the same as the initial external vibration. Moreover, the meniscus can be served as a reservoir, which can gently deliver the external perturbations to the downstream flow and would affect the breakup of the liquid jet. A complete cycle of the jet breakup process at Q_1 = 50 ml/h (50 cSt silicone oil), Q_2 = 2000 ml/h (deionized water), f_e = 400 Hz, and U = 16 V is shown in Fig. 2(b). The breakup of the liquid jet has a regular manner in which the frequency of droplet generation (f_b) is strictly equivalent to the external perturbation frequency (i.e., $f_b = f_e$ = 400 Hz). In this synchronized regime, the resultant droplets are nearly uniform and the jet breakup length keeps almost constant, far different from the jetting regime in the pure AFF process, in which the droplets usually have a certain size distribution and satellite droplets often arise even at a fixed group of process parameters. Moreover, as the applied voltage is slightly increased, the liquid jet breakup length will be decreased, as shown in Fig. 2(c). The dynamic process can be clearly observed through Video S2 of the supplementary material. In these cases, the liquid jet breaks up regularly with the same frequency as that of external perturbations (f_e). Based on the mass conservation law, the droplet size can be precisely predicted by

$$D = \left(\frac{6Q_1}{\pi f_e}\right)^{1/3}, \tag{1}$$

which indicates that the droplet size is only determined by the focused liquid flow rate and the external frequency, but independent of focusing liquid flow rate, structural parameters, and liquid physical properties. Therefore, as demonstrated by the photographs in Fig. 2(c), the resultant droplets keep the same size for different applied voltages.

In experiments, we have obtained the linear relationship between the initial perturbation amplitude and the applied voltage [the inset in Fig. 2(d)] and further measured the vibration amplitude (η) at point P and the jet breakup length (L_b) changing with the applied voltage. In the synchronized regime, the external perturbations propagate along the meniscus to the liquid jet, and the amplitude of perturbations grows along the liquid jet. From the view of temporal linear instability,[14,21] the jet radius R_j changing with time can be predicted by $R_j/R = 1 - (\eta_0/R)e^{\beta t}$, with R being the averaged radius of unperturbed jet, β being the growth rate of perturbations, and η_0 being the initial perturbation amplitude on the jet (here, we assume $\eta_0 = \eta$ for simplification). For a constant Q_1, the averaged jet velocity can be given by $u_j = Q_1/\pi R^2$ and can be determined by Q_1 and Q_2 according to the mass conservation law and the capillary equation of the liquid jet. In particular, one can obtain $R \approx d(1 + Q_2/Q_1)^{-1/2}/2$ if the focusing and focused liquids have nearly the same velocities.[10,34] β is closely related to the flow rates and physical properties of liquids according to the flow focusing principle.[12–14] The breakup time (t_b) can be estimated by taking $R_j/R \to 0$ at the moment when the pinch-off happens, resulting in $\beta t_b = \ln(R/\eta)$. As a result, the breakup length can be written as

$$L_b = u_j t_b = \frac{4(Q_1 + Q_2)}{\pi d^2 \beta} ln\frac{R}{\eta}. \tag{2}$$

It can be seen that for constant Q_1, Q_2, and fixed fluids, the linear relationship between L_b and $\ln \eta$ exists, which is also demonstrated by experimental data in Fig. 2(d). Furthermore, the dimensionless growth rate $\beta^* = \beta R/u_j$ can be estimated to be 0.17, which is comparable to previous studies for the pure AFF case.[14,21] In particular, for an inviscid liquid jet, $\beta^* = 0.34$ can be obtained, suggesting that the

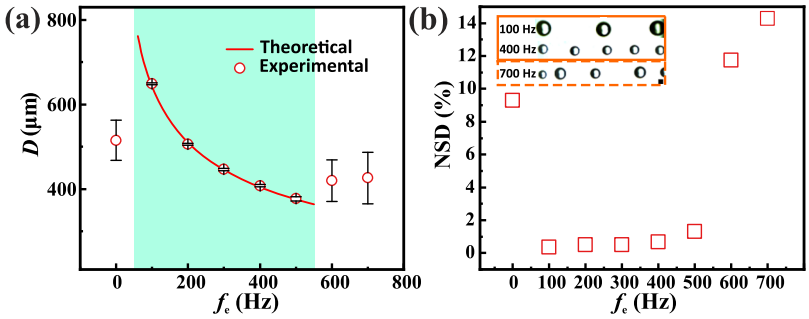

FIG. 3. (a) The variation of droplet size vs excitation frequency (f_e): 0–700 Hz. (b) The normalized standard deviation of collected droplets (the inset indicates the sequence of resultant droplets downstream after the jet breaks up; scale bar: 200 μm). Q_1 = 50 ml/h (50 cSt silicone oil), Q_2 = 2000 ml/h (deionized water), and U = 16 V.

viscosity of focused liquid can suppress the jet instability. Therefore, the magnitude of perturbations only affects the jet breakup length while hardly affects the droplet size.

We further assess the effect of excitation frequency on the droplet size distribution. In a pure AFF process, the liquid jet would break up into droplets with the natural frequency, which can be expressed as $f_n = u_j k^*/2\pi R$, with k^* being the dimensionless wave number of perturbations.[14,21,27] In an unforced Rayleigh-Plateau instability with an inviscid flow assumption, it can be shown that the fastest growing disturbance has a wave number of 0.697. In this work, as the liquid viscosities are considered, k^* = 0.44 can be given, which is little smaller than that in the classical Rayleigh-Plateau instability. As external perturbations are applied, the competition between f_e and f_n appears. Figure 3 presents the variation of droplet diameter vs external perturbation frequency and the normalized standard deviations (NSD) at Q_1 = 50 ml/h, Q_2 = 2000 ml/h, and U = 16 V. In the synchronized regime, the jet breakup follows strict rules as described above, and the droplet size can be well predicted by Eq. (1). The resultant droplets are uniform as the value of NSD is nearly zero. However, for a relatively low or large external frequency, the resultant droplets have a wide size distribution with large NSD (around 10%). We have calculated the averaged value of f_n = 350 Hz in experiments. In this case, u_j, k^*, and R can be estimated to be 0.546 m/s, 0.44 μm, and 90 μm, respectively. Therefore, the natural frequency can be calculated as 420 Hz, which is rather close to the experimental observation and it is just located between minimum and maximum values of critical f_e in the synchronized regime. Therefore, the droplet size can be efficiently manipulated in a wide range of external perturbation frequencies.

It should be emphasized that Eqs. (1) and (2) govern the droplet size and the jet breakup length in this actuated AFF method, and the synchronized regime can be expended for more material combinations and external parametric ranges. As an example, Fig. 4(a) shows the sequence of droplets for higher external frequency at different focusing liquid flow rates Q_2 (2000, 3000, and 4000 ml/h). The value of Q_2 hardly influences the droplet size but can change the range of f_e in the synchronized regime. As f_e increases, the droplet size decreases. Furthermore, the liquid viscosity can directly affect the jet breakup length, even if the other parameters keep constant.[2] As illustrated in Fig. 4(b), the droplets keep nearly the same while the jet breakup length increases dramatically as the liquid viscosity increases. The reason lies in the fact that the perturbation growth rate β in Eq. (2) can be changed by the liquid viscosity.[13,14] Figure 4(c) plots the averaged value of f_n calculated experimentally by statistical data and further presents the range of f_e in the synchronized regime for 10, 50, and 100 cSt silicone oil. In each case, f_n is located within the synchronized regime, and the relationship of $f_b = f_e$ can be strictly satisfied. As the focused liquid viscosity decreases, f_n increases and the maximum value of critical f_e increases as well.

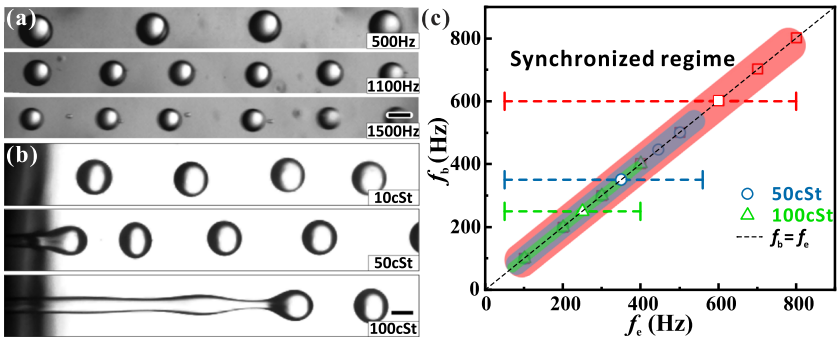

FIG. 4. (a) The sequence of droplets after the jet breaks up in the synchronized regime at f_e = 500, 1100, and 1500 Hz for Q_2 = 2000, 3000, and 4000 ml/h, respectively (50 cSt silicone oil). (b) The breakup of the liquid jet for 10, 50, and 100 cSt silicone oil (Q_2 = 2000 ml/h and f_e = 400 Hz). (c) The averaged value of natural frequency f_n and the range of external frequency f_e in the synchronized regime for 10 (□), 50 (◯), and 100 (△) cSt silicone oil, respectively (Q_2 = 2000 ml/h). In all experiments, Q_1 = 50 ml/h and U = 16 V. Scale bar: 200 μm.

In conclusion, we report a facile but robust method for generating highly uniform and precisely size-controlled droplets by employing external perturbations to the axisymmetric flow focusing in the jetting regime. It is technically feasible to manipulate the droplet size and the liquid jet breakup length at different frequencies and amplitudes of external perturbations. In the synchronized regime, the droplet size is just dependent on the focused liquid flow rate and the perturbation frequency and the liquid jet breakup length can be easily adjusted by the perturbation amplitude. The method also exhibits the ability to further expend the synchronized regime at different conditions. The present work will facilitate the design of active droplet generation for potential applications such as 3D printing, material science, biomedical engineering, and others.

See the supplementary material for more details on cone vibration and jet breakup. Video S1: Harmonic oscillation of the cone under the action of the external disturbance. Video S2: Typical breakup process of active jets with variable disturbance in the synchronized regime.

This work was supported by the Youth Innovation Promotion Association CAS (Grant No. 2018491), the Strategic Priority Research Program of the Chinese Academy of Sciences (Grant No. XDB22040403), the National Natural Science Foundation of China (Grant Nos. 11722222 and 11621202), and the Fundamental Research Funds for the Central Universities.

REFERENCES

[1] G. M. Whitesides, "The origins and the future of microfluidics," Nature **442**, 368 (2006).
[2] S. L. Anna, "Droplets and bubbles in microfluidic devices," Annu. Rev. Fluid Mech. **48**, 285–309 (2016).
[3] P. A. Zhu and L. Q. Wang, "Passive and active droplet generation with microfluidics: A review," Lab Chip **17**, 34–75 (2017).
[4] M. Dejam, H. Hassanzadeh, and Z. X. Chen, "Capillary forces between two parallel plates connected by a liquid bridge," J. Porous Media **18**, 179 (2015).
[5] M. Dejam, "The role of fracture capillary pressure on the block-to-block interaction process," J. Porous Media **21**, 1121 (2018).
[6] S. L. Anna, N. Bontoux, and H. A. Stone, "Formation of dispersions using flow focusing in microchannels," Appl. Phys. Lett. **82**, 364–366 (2003).
[7] H. A. Stone, A. D. Stroock, and A. Ajdari, "Engineering flows in small devices: Microfluidics toward a lab-on-a-chip," Annu. Rev. Fluid Mech. **36**, 381–411 (2004).
[8] M. Azarmanesh, M. Dejam, P. Azizian, G. Yesiloz, A. A. Mohamad, and A. Sanati-Nezhad, "Passive microinjection within high-throughput microfluidics for controlled actuation of droplets and cells," Sci. Rep. **9**, 6723 (2019).
[9] P. Azizian, M. Azarmanesh, M. Dejam, M. Mohammadi, M. Shamsi, A. Sanati-Nezhad, and A. A. Mohamad, "Electrohydrodynamic formation of single and double emulsions for low interfacial tension multiphase systems within microfluidics," Chem. Eng. Sci. **195**, 201–207 (2019).
[10] A. S. Utada, E. Lorenceau, D. R. Link, P. D. Kaplan, H. A. Stone, and D. A. Weitz, "Monodisperse double emulsions generated from a microcapillary device," Science **308**, 537–541 (2005).
[11] Y. K. Jia, Y. K. Ren, L. K. Hou, W. Y. Liu, T. Y. Zhang, X. K. Deng, T. Ye, and H. Y. Jiang, "Electrically controlled rapid release of actives encapsulated in double-emulsion droplets," Lab Chip **18**, 1121–1129 (2018).
[12] A. M. Gañán-Calvo, "Generation of steady liquid microthreads and micron-sized monodisperse sprays in gas streams," Phys. Rev. Lett. **80**, 285 (1998).
[13] A. M. Gañán-Calvo, J. M. Montanero, L. Martin-Banderas, and M. Flores-Mosquera, "Building functional materials for health care and pharmacy from microfluidic principles and flow focusing," Adv. Drug Delivery Rev. **65**, 1447–1469 (2013).
[14] T. Si, F. Li, X. Y. Yin, and X. Z. Yin, "Modes in flow focusing and instability of coaxial liquid–gas jets," J. Fluid Mech. **629**, 1–23 (2009).
[15] A. Barrero and I. G. Loscertales, "Micro-and nanoparticles via capillary flows," Annu. Rev. Fluid Mech. **39**, 89–106 (2007).
[16] S. Yadavali, H. H. Jeong, D. Lee, and D. Issadore, "Silicon and glass very large scale microfluidic droplet integration for terascale generation of polymer microparticles," Nat. Commun. **9**, 1222 (2018).
[17] M. A. Herrada, A. M. Gañán-Calvo, A. Ojeda-Monge, B. Bluth, and P. Riesco-Chueca, "Liquid flow focused by a gas: Jetting, dripping, and recirculation," Phys. Rev. E **78**, 036323 (2008).
[18] A. M. Gañán-Calvo and P. Riesco-Chueca, "Jetting-dripping transition of a liquid jet in a lower viscosity co-flowing immiscible liquid: The minimum flow rate in flow focusing," J. Fluid Mech. **553**, 75–84 (2006).
[19] A. S. Utada, A. Fernandez-Nieves, H. A. Stone, and D. A. Weitz, "Dripping to jetting transitions in coflowing liquid streams," Phys. Rev. Lett. **99**, 094502 (2007).
[20] T. Si, F. Li, X. Y. Yin, and X. Z. Yin, "Spatial instability of coflowing liquid-gas jets in capillary flow focusing," Phys. Fluids **22**, 112105 (2010).
[21] J. M. Gordillo, M. Perez-Saborid, and A. M. Gañán-Calvo, "Linear stability of co-flowing liquid-gas jets," J. Fluid Mech. **448**, 23–51 (2001).
[22] A. Evangelio, F. Campo-Cortes, and J. M. Gordillo, "Simple and double microemulsions via the capillary breakup of highly stretched liquid jets," J. Fluid Mech. **804**, 550–577 (2016).
[23] D. N. Josephides and S. Sajjadi, "Increased drop formation frequency via blackuction of surfactant interactions in flow-focusing microfluidic devices," Langmuir **31**, 1218–1224 (2015).
[24] I. Ziemecka, V. van Steijn, G. J. M. Koper, M. Rosso, A. M. Brizard, J. H. van Esch, and M. T. Kreutzer, "Monodisperse hydrogel microspheres by forced droplet formation in aqueous two-phase systems," Lab Chip **11**, 620–624 (2011).
[25] Z. Z. Chong, S. H. Tan, A. M. Gañán-Calvo, S. B. Tor, N. H. Loh, and N.-T. Nguyen, "Active droplet generation in microfluidics," Lab Chip **16**, 35–58 (2016).
[26] N. Moallemi, R. Li, and K. Mehravaran, "Breakup of capillary jets with different disturbances," Phys. Fluids **28**, 012101 (2016).
[27] K. Mu, T. Si, E. Q. Li, H. Ding, and R. X. Xu, "Numerical study on droplet generation in axisymmetric flow focusing upon actuation," Phys. Fluids **30**, 012111 (2018).
[28] T. Si, H. X. Feng, X. S. Luo, and R. X. Xu, "Formation of steady compound cone-jet modes and multilayered droplets in a tri-axial capillary flow focusing device," Microfluid. Nanofluid. **18**, 967–977 (2015).
[29] T. Si, C. S. Yin, P. Gao, G. B. Li, H. Ding, X. M. He, B. Xie, and R. X. Xu, "Steady cone-jet mode in compound-fluidic electro-flow focusing for fabricating multicompartment microcapsules," Appl. Phys. Lett. **108**, 021601 (2016).
[30] Q. Wu, C. Y. Yang, G. L. Liu, W. H. Xu, Z. Q. Zhu, T. Si, and R. X. Xu, "Multiplex coaxial flow focusing for producing multicompartment janus microcapsules with tunable material compositions and structural characteristics," Lab Chip **17**, 3168–3175 (2017).
[31] Q. Wu, C. Y. Yang, J. X. Yang, F. S. Huang, G. L. Liu, Z. Q. Zhu, T. Si, and R. X. Xu, "Photopolymerization of complex emulsions with irregular shapes fabricated by multiplex coaxial flow focusing," Appl. Phys. Lett. **112**, 071601 (2018).
[32] Z. Q. Zhu, Q. Wu, S. Y. Han, W. H. Xu, F. J. Zhong, S. Yuan, P. Dwivedi, T. Si, and R. X. Xu, "Rapid production of single-and multi-compartment polymeric microcapsules in a facile 3d microfluidic process for magnetic separation and synergistic delivery," Sens. Actuators, B **275**, 190–198 (2018).
[33] S. B. Li, R. Yang, K. Mu, X. S. Luo, and T. Si, "Thermal effects on the instability of coaxial liquid jets in the core of a gas stream," Phys. Fluids **31**, 032106 (2019).
[34] Z. Q. Zhu, T. Si, and R. X. Xu, "Microencapsulation of indocyanine green for potential applications in image-guided drug delivery," Lab Chip **15**, 646–649 (2015).